JOURNAL OF THERMOPHYSICS AND HEAT TRANSFER
Vol. 27, No. 2, April–June 2013

Natural-Convection Flow of Nanofluids Over Vertical Cone Embedded in Non-Darcy Porous Media

A. Noghrehabadi,* A. Behseresht,† and M. Ghalambaz‡
Shahid Chamran University of Ahvaz, Ahvaz 61357, Iran
and
J. Behseresht§
University of Texas at Austin, Houston 78712, Texas

DOI: 10.2514/1.T3965

In this paper, non-Darcy flow and natural convection over a vertical cone embedded in a porous medium saturated with a nanofluid is studied using the Forchheimer-extended Darcy law. The model used for the nanofluid incorporates the effects of Brownian motion and thermophoresis. An analytical technique, similarity solution method, is used to convert the governing equations into a set of ordinary differential equations, and then numerically solved using the finite difference method. The effect of non-Darcy parameter and nanofluid parameters on the velocity, temperature, and nanoparticles volume fraction profiles, as well as on the two important parameters of heat and mass transfer, i.e., reduced Nusselt and Sherwood numbers, are discussed. The results show that an increase in the non-Darcy parameter decreases the velocity profiles, whereas it would increase the temperature and concentration profiles. Simulation results also show that an increase in the non-Darcy parameter would decrease the reduced Nusselt and Sherwood numbers, whereas an increase of Lewis number would increase the reduced Nusselt and Sherwood numbers.

Nomenclature

D_B	=	Brownian diffusion coefficient
D_T	=	thermophoretic diffusion coefficient
F	=	rescaled nanoparticle volume fraction, nanoparticle concentration
g	=	gravitational acceleration vector
K	=	permeability of porous medium
k	=	thermal conductivity
k_m	=	effective thermal conductivity of the porous medium
Le	=	Lewis number
Nb	=	Brownian motion parameter
ND	=	non-Darcy parameter
Nr	=	buoyancy ratio
Nt	=	thermophoresis parameter
P	=	pressure
Ra_x	=	local Rayleigh number
S	=	dimensionless stream function
T	=	temperature
T_∞	=	ambient temperature
T_W	=	surface temperature of the vertical cone
U	=	reference velocity
u, v	=	Darcy velocity components
(x, y)	=	Cartesian coordinates
α_m	=	thermal diffusivity of porous media
β	=	volumetric expansion coefficient of fluid
γ	=	cone half-angle
ε	=	porosity
η	=	dimensionless distance
θ	=	dimensionless temperature
μ	=	viscosity of fluid
ρ_f	=	fluid density
ρ_p	=	nanoparticle mass density
$(\rho c)_f$	=	heat capacity of the fluid
$(\rho c)_m$	=	effective heat capacity of porous medium
$(\rho c)_p$	=	effective heat capacity of nanoparticle material
τ	=	parameter defined by Eq. (7)
φ	=	nanoparticle volume fraction
φ_∞	=	ambient nanoparticle volume fraction
φ_w	=	nanoparticle volume fraction at the surface of the vertical cone
ψ	=	stream function

Received 5 June 2012; revision received 13 November 2012; accepted for publication 11 December 2012; published online 14 March 2013.

*Assistant Professor, Department of Mechanical Engineering; noghrehabadi@scu.ac.ir. (Corresponding Author).

†Graduate M.S., Department of Mechanical Engineering; behseresht.ali@gmail.com.

‡Ph.D. Student, Department of Mechanical Engineering; m.ghalambaz@gmail.com.

§Ph.D., Reservoir Engineer, Marathon Oil Corporation; jbehseresht@utexas.edu.

I. Introduction

IMPROVING the performance of cooling systems is essential to many industrial applications, for example, high performance cooling systems where energy-efficient heat transfer fluids are required. However, inherently low thermal conductivity of fluids is a primary limitation in developing highly efficient cooling systems. Nanofluids were recently introduced to resolve the latter limitation [1]. Nanofluids are produced by suspending nanoparticles, metallic or nonmetallic particles of nanometer dimensions, in traditional heat transfer fluids such as water, oil, and ethylene glycol. In fact, a very small amount of uniformly dispersed guest nanoparticles can dramatically improve the thermal properties of host fluids [1].

The analysis and simulation of natural convection in saturated porous media has many important engineering and geophysical applications. For example, the prediction of natural convection heat transfer characteristics from heated bodies embedded in a porous medium is crucial to the design of canisters for nuclear wastes disposal [2].

An inevitable part of any convection heat transfer analysis within porous media is the effect of fluid flow within the media. Fluid flow in porous media is governed not only by the magnitude of the potential gradient across the media but also the drag forces experienced by the fluid within the porous media. Generally, there are two main types of drag forces against fluid flow in porous media: 1) surface drag (friction), and 2) form drag (due to solid obstacles).

The Darcy equation in its simple linear form [3]

$$\nabla P = -\frac{\mu}{K} V \tag{1}$$

accounts for the surface drag only. That is why Darcy equation is valid only at small enough flow rates owing to the fact that at very low velocities, i.e., Reynolds number < 1, form drag is much less than surface drag and thus can be neglected. Here, V is superficial velocity, K is effective permeability, and P and μ are the pressure and dynamic viscosity of the flowing phase, respectively. For higher velocities, i.e., Reynolds number > 1, drag force becomes comparable to the surface drag. Forchheimer added a modification term to Darcy equation to account for the pressure drop due to the form drag [3], which was ignored by Darcy. The Forchheimer-extended Darcy equation is as follows,

$$\nabla P = -\frac{\mu}{K}V - c_F K^{-\frac{1}{2}}\rho_f |V|V \tag{2}$$

where c_F is a dimensionless form drag constant, and ρ_f is the density of the flowing phase. Forchheimer equation considers two contributions to the pressure drop: 1) surface drag and 2) form drag. The linear part of the equation (the first term on the right hand side) accounts for the surface drag pressure drop. The form drag pressure drop is described by the nonlinear term known as the Forchheimer term.

The problem of natural convection around a cone embedded in a porous medium at high Rayleigh numbers has been numerically analyzed by Cheng et al. [2]. Yih [4] numerically investigated the effect of uniform lateral mass flux on natural convection around a cone embedded in a saturated porous medium using Keller box method. He found that the mass flux parameter has a more significant effect on the local Nusselt number for constant surface temperature case than that of a constant heat flux case. Moreover, the radiation effect on mixed convection across an isothermal cone in porous media was investigated by Yih [5]. Yih [5] reported that an increase in the radiation parameter would increase the local Nusselt number. Grosan et al. [6] studied a free convection boundary layer over a vertical cone embedded in a porous medium saturated with non-Newtonian fluid subject to internal heat generation using a finite difference method. They showed that the local heat transfer would decrease with the presence of a heat generation source within the porous medium. Likewise, Ramanaiah and Malarvizhi [7] studied the free convection about a wedge and a cone subjected to mixed thermal boundary condition. Later, Chamkha et al. [8] investigated the steady free convection flow over a truncated cone embedded in a porous medium saturated with pure or saline water at low temperatures. Sohouli et al. [9] analyzed the problem of natural convection of Darcian fluid across a vertical full cone embedded in porous media using the Homotopy analysis method. The natural convection heat and mass transfer from a vertical truncated cone in a porous medium saturated with a non-Newtonian fluid has been investigated using cubic spline collocation method by Cheng [10]. The important finding of the study of Cheng [10] was that the heat transfer would decrease with an increase of power-law index of the fluids. In another work Cheng [11] studied the Soret and Dufour effects on natural convection from a vertical cone in a porous medium. Most of the mentioned studies (Cheng et al. [2], Yih [4], Grosan et al. [6], Chamkha et al. [8] and Cheng [10,11]) have considered the fluid flow in porous media as a Darcy flow. However, some studies in the literature considered the non-Darcy flow in porous media. Vasantha et al. [12] considered the problem of non-Darcy natural convection over a slender vertical frustum of a cone in a saturated porous medium. They solved the system of equations using a finite difference scheme. Later, a unified similarity transformation for free, forced, and mixed convection in Darcy and non-Darcy porous media was analyzed by Nakayama and Pop [13]. Prior to that work [13], Nakayama et al. [14] had proposed an integral treatment to analyze non-Darcy free convection over a vertical flat plate and cone embedded in a fluid-saturated porous medium. They reported a good agreement between the results of their proposed method with the exact solution. They also showed that increase of Forchheimer term tends to increase the dimensionless temperature while decreasing the local Nusselt number. Cheng [15] studied the non-Darcy natural convection heat and mass transfer from a vertical wavy surface within a saturated porous medium and reported that increasing the modified Grashof number would decrease the heat and mass transfer rate.

Convectional fluid flow and heat transfer via natural convection over embedded bodies in porous media are extensively discussed in the literature. However, few studies have been performed on flow and heat transfer of nanofluids. Specifically, nanofluid heat transfer in porous media is an area that certainly demands further studies.

Mixed convection boundary-layer flow from a vertical flat plate embedded in a porous medium filled with nanofluids was studied by Ahmad and Pop [16]. Later, Hady et al. [17] investigated the natural convective boundary-layer flow from a vertical isothermal cone embedded in a porous medium saturated with a nanofluid. However, both models incorporated only the nanoparticle volume fraction parameter.

The boundary-layer flow in the porous media saturated with a nanofluid has recently been analyzed by Nield and Kuznetsov [18]. Their nanofluid model employs the Darcy model and incorporates the effect of Brownian motion and thermophoresis. They reported that the variation of the Brownian motion and thermophoresis parameters affect the reduced Nusselt number. Following the work of Nield and Kuznetsov [18], Gorla et al. [19] as well as Rashad et al. [20] studied heat transfer enhancement of nanofluids over embedded bodies for Darcy flows.

The objective of the present paper is to analyze the steady natural convection flow of a nanofluid past an isothermal vertical cone embedded in saturated non-Darcy porous media. The nanofluid model, used in the present study, incorporates dynamic effects of nanoparticles including Brownian motion and thermophoresis. A similarity solution depending on the buoyancy ratio parameter (Nr), Lewis number (Le), Brownian motion parameter (Nb), thermophoresis parameter (Nt), and non-Darcy parameter (ND) is obtained. The dependency of the local Nusselt and Sherwood numbers on these five parameters is numerically investigated.

II. Mathematical Formulations

Consider the two-dimensional steady natural convection boundary-layer flow past along a vertical full cone placed in a non-Darcy porous medium saturated with nanofluid. The cone surface is imposed to a constant temperature T_w. The coordinate system is chosen such that the x axis is aligned with the flow on the surface of the cone. A schematic of the physical model and coordinate system are shown in Fig. 1. As shown in Fig. 1, there are three distinct boundary layers namely, the hydrodynamic boundary layer, the thermal boundary layer, and the nanoparticle concentration boundary layer. It is assumed that the nanoparticle volume fraction (φ) at the wall surface ($y = 0$) has a fixed value of φ_w. The ambient values of T

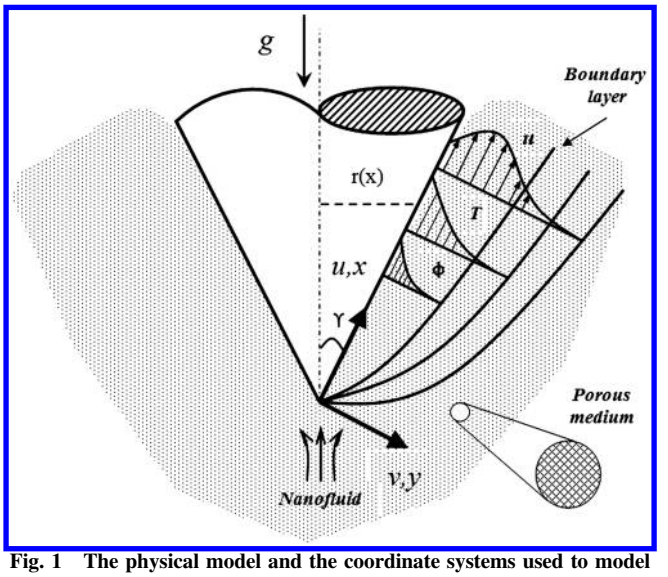

Fig. 1 The physical model and the coordinate systems used to model convective heat transfer around a vertical cone embedded inside a homogeneous porous media saturated with a nanofluid.

and φ, as y tends to infinity, are denoted by T_∞ and φ_∞, respectively. The flow in the porous medium, with porosity ε and permeability K is considered as non-Darcy flow, and the Oberbeck–Boussinesq approximation is applied. Furthermore, it is assumed that the porous medium is homogeneous and in local thermal equilibrium.

Applying the standard boundary layer approximations, the steady-state conservation of total mass, Eq. (3), momentum, Eq. (4), and energy, Eq. (5), as well as conservation of nanoparticles for nanofluids, Eq. (6), are as follows [3] and [18],

$$\frac{\partial(ru)}{\partial x}+\frac{\partial(rv)}{\partial y}=0 \tag{3}$$

$$\frac{\partial p}{\partial y}=0 \tag{4a}$$

$$\frac{\mu}{K}u+\frac{c_F\rho_{f_\infty}}{\sqrt{K}}u^2=\begin{bmatrix}-\left(\frac{\partial p}{\partial x}-(1-\phi_\infty)\beta g\rho_{f_\infty}\cos\gamma(T-T_\infty)\right)\\ -(\rho_P-\rho_{f_\infty})g\cos\gamma(\phi-\phi_\infty)\end{bmatrix} \tag{4b}$$

$$u\frac{\partial T}{\partial x}+v\frac{\partial T}{\partial y}=\alpha_m\nabla^2T+\tau\left[D_B\frac{\partial\varphi}{\partial y}\frac{\partial T}{\partial y}+\frac{D_T}{T_\infty}\left(\frac{\partial T}{\partial y}\right)^2\right] \tag{5}$$

$$\frac{1}{\varepsilon}\left[u\frac{\partial\phi}{\partial x}+v\frac{\partial\phi}{\partial y}\right]=D_B\frac{\partial^2\phi}{\partial y^2}+\left(\frac{D_T}{T_\infty}\right)\frac{\partial^2T}{\partial y^2} \tag{6}$$

α_m and τ, in the preceding equations, are defined as:

$$\alpha_m=\frac{k_m}{(\rho c)_f},\qquad \tau=\frac{\varepsilon(\rho c)_p}{(\rho c)_f} \tag{7}$$

Based on the problem description, the boundary conditions are:

$$v=0,\qquad T=T_w,\qquad \phi=\phi_w,\quad \text{at } y=0, x\geq 0 \tag{8}$$

$$u=v=0,\qquad T\to T_\infty,\qquad \phi\to\phi_\infty,\quad \text{at } y\to\infty \tag{9}$$

It is assumed that the thermal boundary layer is thin; therefore, r can be approximated by the local radius of the cone. Equations (4a) and (4b) are simplified using cross-differentiation, and the continuity equation will also be satisfied by introducing a stream function, (ψ):

$$u=\frac{1}{r}\frac{\partial\psi}{\partial y},\qquad v=-\frac{1}{r}\frac{\partial\psi}{\partial x} \tag{10}$$

The governing differential equations, Eqs. (3–6), are then reduced to the following three equations:

$$\frac{1}{r}\frac{\partial^2\psi}{\partial y^2}+\frac{c_F\rho_{f\infty}\sqrt{K}}{\mu}\frac{\partial}{\partial y}\left(\frac{1}{r}\frac{\partial\psi}{\partial y}\right)^2=\frac{(1-\phi_\infty)\rho_{f\infty}\beta gK\cos\gamma}{\mu}\frac{\partial T}{\partial y}-\frac{(\rho_p-\rho_{f\infty})gK\cos\gamma}{\mu}\frac{\partial\phi}{\partial y} \tag{11}$$

$$\frac{1}{r}\frac{\partial\psi}{\partial y}\frac{\partial T}{\partial x}-\frac{1}{r}\frac{\partial\psi}{\partial x}\frac{\partial T}{\partial y}=\alpha_m\frac{\partial^2T}{\partial y^2}+\tau\left[D_B\frac{\partial\phi}{\partial y}\frac{\partial T}{\partial y}+\frac{D_T}{T_\infty}\left(\frac{\partial T}{\partial y}\right)^2\right] \tag{12}$$

$$\frac{1}{\varepsilon}\left(\frac{1}{r}\frac{\partial\psi}{\partial y}\frac{\partial\phi}{\partial x}-\frac{1}{r}\frac{\partial\psi}{\partial x}\frac{\partial\phi}{\partial y}\right)=D_B\frac{\partial^2\phi}{\partial y^2}+\left(\frac{D_T}{T_\infty}\right)\frac{\partial^2T}{\partial y^2} \tag{13}$$

Here, the local Rayleigh number (Ra_x) is defined as:

$$Ra_x=\frac{(1-\phi_\infty)\rho_{f\infty}\beta gKx\cos\gamma(T_w-T_\infty)}{\mu\alpha_m} \tag{14}$$

By introducing the similarity variable η as,

$$\eta=\frac{y}{x}Ra_x^{\frac{1}{2}} \tag{15}$$

and the dimensionless similarity quantities S, f, and θ as,

$$S=\frac{\psi}{\alpha_m rRa_x^{\frac{1}{2}}},\qquad f=\frac{\phi-\phi_\infty}{\phi_w-\phi_\infty},\qquad \theta=\frac{T-T_\infty}{T_w-T_\infty} \tag{16}$$

and also by considering the local radius as

$$r=x\sin\gamma \tag{17}$$

Equations (11–13) can be written as three ordinary differential equations, Eqs. (18–20),

$$S''(1+\text{ND}.S')-\theta'+Nr.f'=0 \tag{18}$$

$$\theta''+\frac{3}{2}S\theta'+Nb.f'.\theta'+Nt(\theta')^2=0 \tag{19}$$

$$f''+\frac{3}{2}Le.S.f'+\frac{Nt}{Nb}\theta''=0 \tag{20}$$

subject to the following boundary conditions,

$$\eta=0\colon\ S=0,\qquad \theta=1,\qquad f=1 \tag{21a}$$

$$\eta\to\infty\colon\ S'=0,\qquad \theta=0,\qquad f=0 \tag{21b}$$

Where:

$$Nr=\frac{(\rho_p-\rho_{f\infty})(\phi_w-\phi_\infty)}{(1-\phi_\infty)\rho_{f\infty}\beta(T_w-T_\infty)} \tag{22a}$$

$$Nb=\frac{\varepsilon(\rho c)_pD_B(\phi_w-\phi_\infty)}{(\rho c)_f\alpha_m} \tag{22b}$$

$$Nt=\frac{\varepsilon(\rho c)_pD_T(T_w-T_\infty)}{(\rho c)_f\alpha_mT_\infty} \tag{22c}$$

$$Le=\frac{\alpha_m}{\varepsilon D_B} \tag{22d}$$

$$\text{ND}=\frac{2\rho_{f\infty}c_F\sqrt{K}\alpha_mRa_x}{\mu x} \tag{22e}$$

Two important heat transfer parameters, the local Nusselt number (Nu_x) and the local Sherwood number (Sh_x), are defined as [20]:

$$Nu_x=\frac{q_Wx}{k(T_W-T_\infty)} \tag{23}$$

$$Sh_x=\frac{q_mx}{D_B(\phi_W-\phi_\infty)} \tag{24}$$

where q_w and q_m are the wall heat flux and mass flux, respectively.

Using similarity transforms introduced in Eq. (16), the reduced Nusselt number, $-\theta'(0)$, and reduced Sherwood number, $-f'(0)$, are obtained as follows,

$$Nu_x Ra_x^{-\frac{1}{2}} = Nu_r = -\theta'(0) \tag{25}$$

$$Sh_x Ra_x^{-\frac{1}{2}} = Sh_r = -f'(0) \tag{26}$$

III. Solution

The system of Eqs. (18–20) subject to the boundary conditions, Eq. (21), is numerically solved for various ranges of Nr, Nb, Nt, ND, and selected values of Le. The numerical results were obtained using finite difference method based on collocation points and Newton's method [21,22]. Highly accurate solutions, with a relative tolerance of 10^{-6}, were achieved using an adaptive mesh scheme. An important criterion for the success of this numerical approach is to choose an appropriate finite value of η_∞. Thus, in order to estimate the realistic value of η_∞, the solution process begins with initial guess value of $\eta_\infty = 6$, and the Eqs. (18–20) are solved subject to the boundary conditions, i.e., Eq. (21). The solution process is repeated to update value of η_∞ until further changes (increment) in η_∞ does not lead to any changes in the values of results or, in other words, the results are independent of the value of η_∞.

Figure 2 shows the effect of variation of η_∞ on the reduced Nusselt number and reduced Sherwood number. In this figure, the finite value of η_∞ is chosen to be in the range of $4 < \eta_\infty < 10$, which is in accordance with the standard practice in the boundary layer analysis. This figure depicts that as the finite value of η_∞ increases, the reduced Nusselt number and the reduced Sherwood number tend to become a fixed value. It is found that for small values of non-Darcy parameter, i.e., ND = 0, 0.1, 1, the finite value of η_∞ is 6, for medium value of non-Darcy parameter, i.e., ND = 10, the finite value of $\eta_\infty = 10$ and for large value of non-Darcy parameter, i.e., ND = 100, the finite value of $\eta_\infty = 12$ are comparatively adequate to obtain an accurate solution.

By neglecting the effects of thermophoresis, Brownian motion, buoyancy ratio parameters ($Nt = Nb = Nr = 0$) and non-Darcy effects (ND = 0), in the model of present study, we simulate a pure fluid case, which was also studied by Cheng et al. [2] and Yih [4]. The latter results are then used to evaluate the accuracy of present solution. The value of $-\theta'(0)$ is calculated as 0.7685 in the work of Cheng et al. [2], and 0.7686 in the works of Yih [4], although we obtained this value as 0.76859 in the present work. Furthermore, the temperature profile of the present solution is compared with the results of Yih [4] in Fig. 3. The obtained value of $-\theta'(0)$ as well as the results of Fig. 3 show excellent agreement between the results of present study and the results reported by Yih [4] and Cheng et al. [2].

IV. Results and Discussion

In the present study, the values of non-Darcy parameter (ND) are chosen to be in the range of $0 < \text{ND} < 10$ to clearly show the effect of this parameter on the dimensionless velocity, temperature and concentration profiles as well as reduced Nusselt and Sherwood numbers. Most nanofluids reported in the literatures have large values of Lewis number, i.e., $Le > 1$ [18–20,23,24]. Hence, the selected values of $Le = 10$ and $Le = 25$ are used here. The same values of Nr, Nb, and Nt as those adopted by Rashad et al. [20] are used in the present study. The latter values allow us to evaluate the effect of non-Darcy parameter (ND), compared to the work of Rashad et al. [20], who neglect the non-Darcy effect in modeling natural convection boundary layer of a non-Newtonian fluid about a permeable vertical cone embedded in a porous medium saturated with a nanofluid.

The main parameter of interest in the present study is the heat transfer enhancement of nanofluids. Therefore, the results of reduced Nusselt number are shown in Table 1. The values are reported for a selected combination of Nt, Nb, and Nr and four values of non-Darcy parameter (ND = 0, 0.1, 1, and 10) when $Le = 10$. Table 1 shows that an increase in Brownian motion parameter would decrease

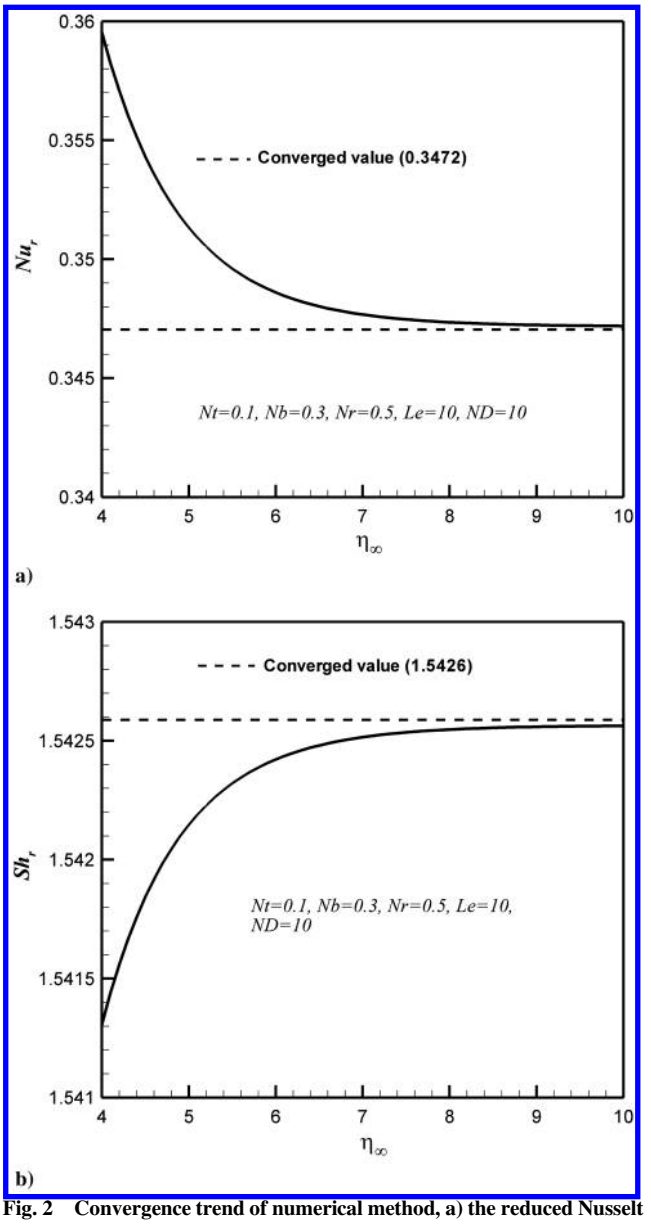

Fig. 2 Convergence trend of numerical method, a) the reduced Nusselt number, b) the reduced Sherwood number.

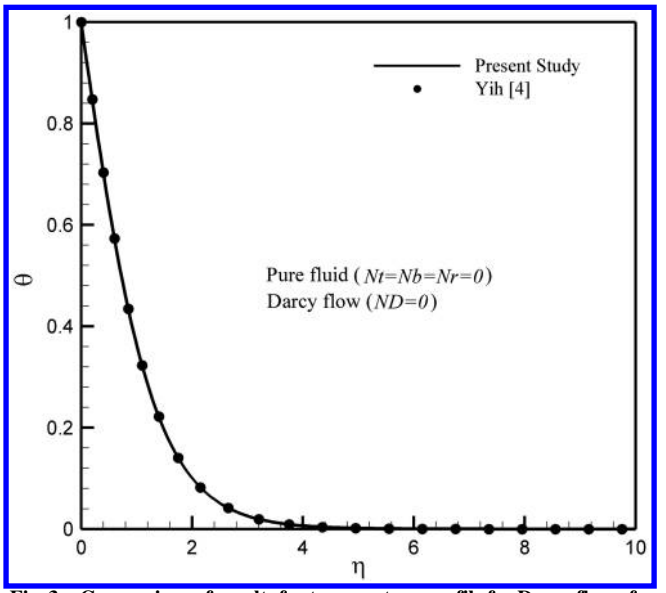

Fig. 3 Comparison of results for temperature profile for Darcy flow of a pure fluid.

Table 1 The reduced Nusselt number for different values of Nb, Nt, Nr, ND, and for $Le = 10$

		$-\theta'(0)$							
		$Nr = 0.1$				$Nr = 0.5$			
Nb	Nt	ND = 0	ND = 0.1	ND = 1	ND = 10	ND = 0	ND = 0.1	ND = 1	ND = 10
	0.1	0.6672	0.6563	0.5928	0.4332	0.5940	0.5865	0.5391	0.4032
	0.2	0.6401	0.6296	0.5685	0.4152	0.5629	0.5559	0.5115	0.3832
0.1	0.3	0.6145	0.6044	0.5456	0.3981	0.5343	0.5277	0.4860	0.3647
	0.4	0.5904	0.5807	0.5239	0.3821	0.5079	0.5018	0.4624	0.3475
	0.5	0.5676	0.5582	0.5035	0.3669	0.4835	0.4778	0.4406	0.3315
	0.1	0.6176	0.6074	0.5484	0.4004	0.5553	0.5481	0.5029	0.3751
	0.2	0.5932	0.5834	0.5264	0.3840	0.5307	0.5238	0.4806	0.3585
0.2	0.3	0.5702	0.5607	0.5057	0.3685	0.5077	0.5011	0.4598	0.3430
	0.4	0.5484	0.5392	0.4860	0.3539	0.4862	0.4800	0.4403	0.3284
	0.5	0.5277	0.5188	0.4674	0.3400	0.4662	0.4602	0.4221	0.3148
	0.1	0.5705	0.5611	0.5063	0.3695	0.5154	0.5087	0.4662	0.3472
	0.2	0.5482	0.5391	0.4862	0.3544	0.4938	0.4873	0.4465	0.3324
0.3	0.3	0.5271	0.5183	0.4671	0.3402	0.4735	0.4672	0.4280	0.3184
	0.4	0.5070	0.4985	0.4491	0.3267	0.4545	0.4484	0.4106	0.3054
	0.5	0.4880	0.4797	0.4319	0.3139	0.4365	0.4307	0.3943	0.2930
	0.1	0.5265	0.5178	0.4671	0.3406	0.4773	0.4709	0.4312	0.3208
	0.2	0.5060	0.4975	0.4485	0.3268	0.4578	0.4516	0.4134	0.3073
0.4	0.3	0.4865	0.4783	0.4310	0.3137	0.4394	0.4335	0.3966	0.2946
	0.4	0.4680	0.4601	0.4143	0.3012	0.4221	0.4164	0.3808	0.2827
	0.5	0.4505	0.4428	0.3985	0.2895	0.4058	0.4002	0.3659	0.2714
	0.1	0.4855	0.4774	0.4305	0.3138	0.4413	0.4353	0.3984	0.2960
	0.2	0.4666	0.4587	0.4134	0.3010	0.4235	0.4177	0.3821	0.2837
0.5	0.3	0.4486	0.4410	0.3972	0.2889	0.4067	0.4011	0.3667	0.2721
	0.4	0.4315	0.4242	0.3818	0.2775	0.3909	0.3855	0.3523	0.2611
	0.5	0.4154	0.4082	0.3673	0.2666	0.3759	0.3707	0.3386	0.2507

the reduced Nusselt number. Similarly, an increase in buoyancy ratio parameter would decrease the reduced Nusselt number. Moreover, this table shows that the reduced Nusselt number decreases as the thermophoresis parameter increases. Furthermore, the reduced Nusselt number decreases as the non-Darcy parameter increases from ND = 0 (Darcy assumption) to ND = 0.1, 1 and 10 (non-Darcy assumption).

Figures 4–6 show the influence of the non-Darcy parameter (ND) on the dimensionless velocity, temperature, and concentration profiles, respectively. In these figures, the values of four other parameters namely Nr, Nb, Nt, and Le are fixed. As seen, the increase of non-Darcy parameter would decrease the velocity profiles. Conversely, the temperature and concentration profiles increase with the non-Darcy parameter ND. The reason for this behavior is that increasing the non-Darcy parameter, i.e., Forchheimer term, would also increase the pressure drop associated with form drag. This means that, assuming the velocity is fixed, a system with a larger Forchheimer's coefficient exhibits a larger pressure drop due to form drag forces. Equivalently, for a fixed-pressure gradient, when the non-Darcy parameter, i.e., Forchheimer term, increases, velocity would decrease. This dependence between Forchheimer term and velocity is also observed in Fig. 4. This figure shows that an increase in Forchheimer parameter decreases the magnitude and curvature of the velocity profiles in near-wall regions. However, the boundary layer thickness increases with the Forchheimer parameter. When velocity decreases, convective heat transfer coefficient also decreases; consequently, the decreasing in convective heat transfer coefficient would lead to less heat dissipation, and thus the temperature would rise. Figure 5 obviously exhibits an increasing temperature profile as the non-Darcy parameter is increased. Furthermore, increase of the non-Darcy parameter increases the concentration profile as shown in Fig. 6. Such behavior was also reported by Cheng et al. [25] where they performed an experimental study of non-Darcian effects on free convection in a saturated porous medium. Moreover, the increase in

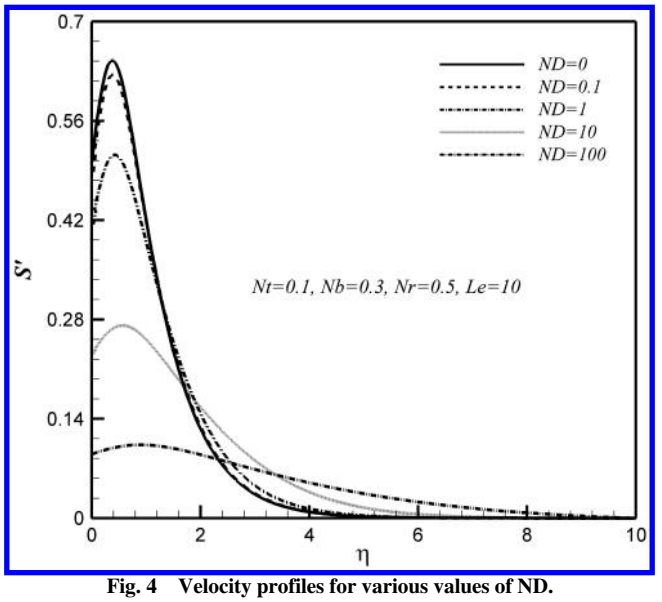

Fig. 4 Velocity profiles for various values of ND.

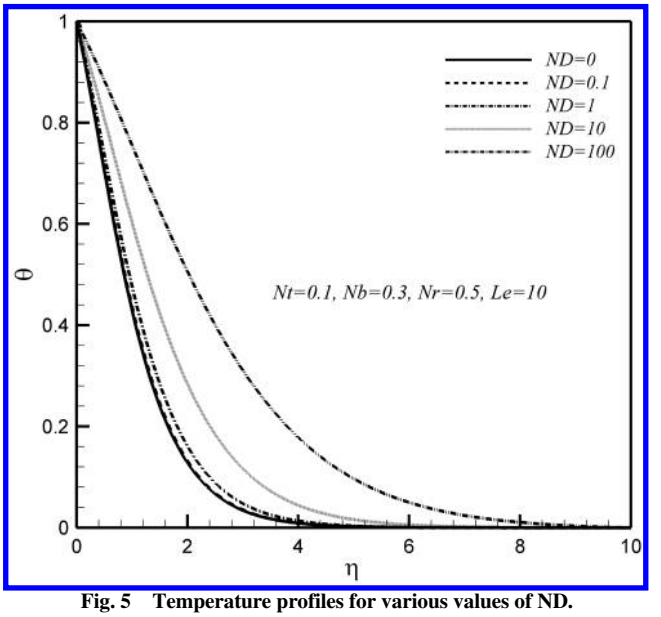

Fig. 5 Temperature profiles for various values of ND.

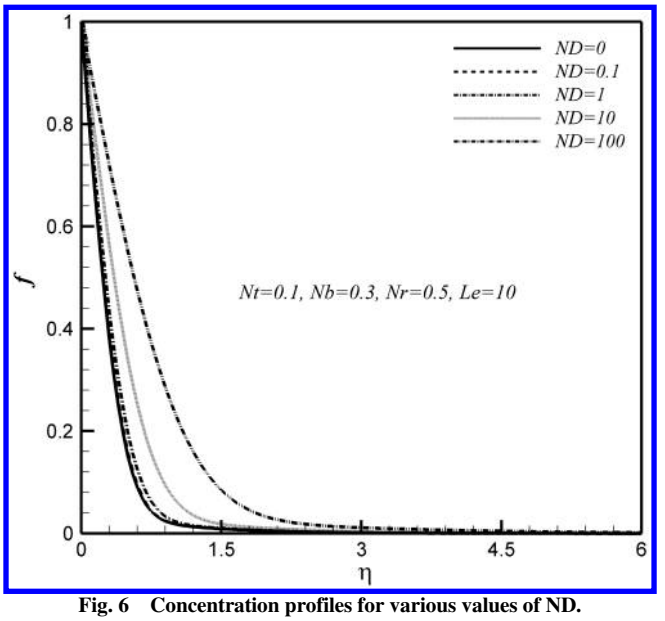

Fig. 6 Concentration profiles for various values of ND.

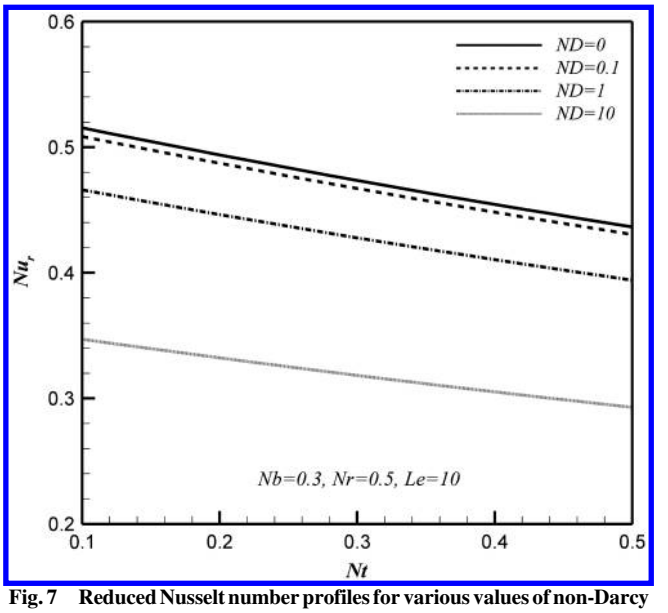

Fig. 7 Reduced Nusselt number profiles for various values of non-Darcy parameter (ND) and thermophoresis parameter (Nt) for $Le = 10$.

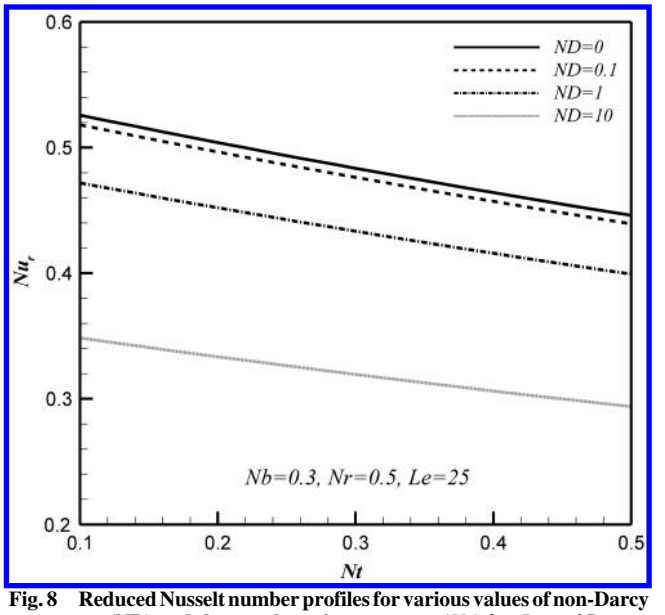

Fig. 8 Reduced Nusselt number profiles for various values of non-Darcy parameter (ND) and thermophoresis parameter (Nt) for $Le = 25$.

the non-Darcy parameter has a significant effect on the shape of velocity, temperature, and concentration profiles. As Figs. 4–6 obviously show, the curvature of velocity, temperature, and concentration profiles are reduced by increase of the non-Darcy parameter.

The Brownian motion parameter can be described as the ratio of nanoparticle diffusion due to the Brownian motion to the thermal diffusion within a nanofluid. Based on the Einstein–Stokes equation [26], the Brownian motion diffusion is inversely proportional to the particle diameter [26]. Hence, as the particle diameter decreases, the Brownian motion diffusion increases.

The Brownian motion parameter can be increased by either increasing the difference between nanoparticle volume fraction at the wall and that in far field, or increasing the Brownian coefficient parameter for a specific porous medium, base fluid type, and nanoparticle type. Increase of Brownian motion parameter increases the nanoparticle diffusion, which would increase the dimensionless velocity profiles.

Thermophoresis parameter (Nt) is defined as the ratio of nanoparticle diffusion due to the thermophoresis effect to the thermal diffusion within a nanofluid. The difference between the momentums that a solid particle receives from hot and cold fluid atoms, owing to a temperature gradient, results in a net force that is known as thermophoresis force [27]. Buongiorno [26] has reported that solid nanoparticles within a nanofluid experience a force in a direction opposite to that of the imposed temperature gradient. Therefore, the nanoparticles tend to move from hot to cold. The obtained results show that increase of Nt increases the magnitude of velocity, temperature, and concentration profiles. However, the increase of velocity profile is not significant. The atoms that are near the hot wall carry more momentum than those far from the wall, i.e., colder regions. Therefore, it is expected that increase of Nt increases the force on the nanoparticles away from the hot wall and thus increases the diffusion of nanoparticles within the nanofluid. The increase of thermophoresis force increases the diffusion of nanoparticles into the nanofluid and consequently increases the non-dimensional velocity profiles. The thermophoresis parameter is independent of particle diameter in the case of particles with very small size [26]. As Nt increases the non dimensional temperature due to heat transfer increases.

The nondimensional profiles of reduced Nusselt and Sherwood numbers are shown in Figs. 7–10 for different values of thermophoresis parameter (Nt) and four values of non-Darcy parameter (ND = 0, 0.1, 1 and 10) when the buoyancy-ratio parameter (Nr), Brownian motion parameter (Nb), and Lewis number (Le) are fixed.

Figures 7 and 8 show the variation of reduced Nusselt number for different values of Nt and ND in two cases of $Le = 10$ and $Le = 25$, respectively. These figures depict that increase of non-Darcy parameter decreases the magnitude of reduced Nusselt number. In addition, increase of thermophoresis parameter decreases the magnitude of reduced Nusselt number, whereas an increase in Lewis number increases the magnitude of reduced Nusselt number.

Increase of non-Darcy parameter decreases the magnitude of temperature gradient on the wall surface. As mentioned earlier, the increase of non-Darcy parameter decreases the velocity, and thus it decreases the reduced Nusselt number (Figs. 7 and 8). This is in good agreement with the reported results by Cheng et al. [25]. They have experimentally found that non-Darcian effects tend to decrease the heat transfer and increase the temperature distribution in a porous medium [25].

Figures 9 and 10 depict the variation of reduced Sherwood number for different values of Nt and ND for two cases of $Le = 10$ and $Le = 25$, respectively. These figures depict that increase of non-Darcy parameter decreases the magnitude of reduced Sherwood number. On the other hand, the variation of thermophoresis parameter does not exhibit a significant effect on the reduced Sherwood number. Increase of Lewis number, however, increases the magnitude of reduced Sherwood number.

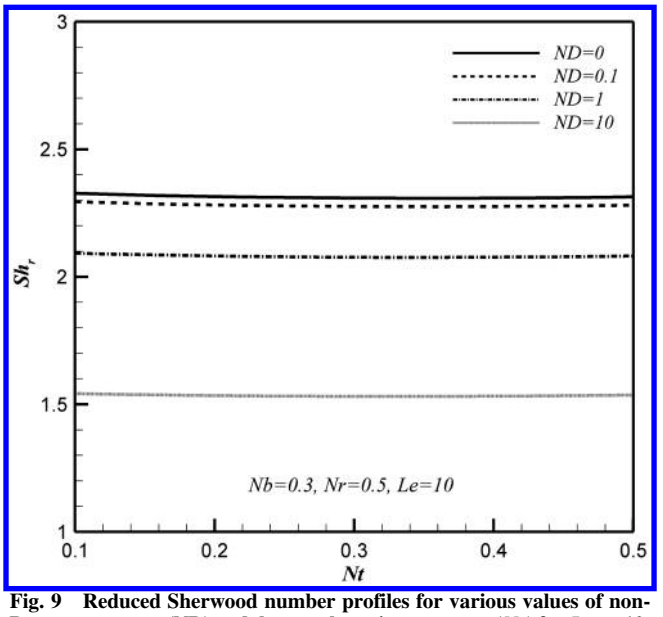

Fig. 9 Reduced Sherwood number profiles for various values of non-Darcy parameter (ND) and thermophoresis parameter (Nt) for $Le = 10$.

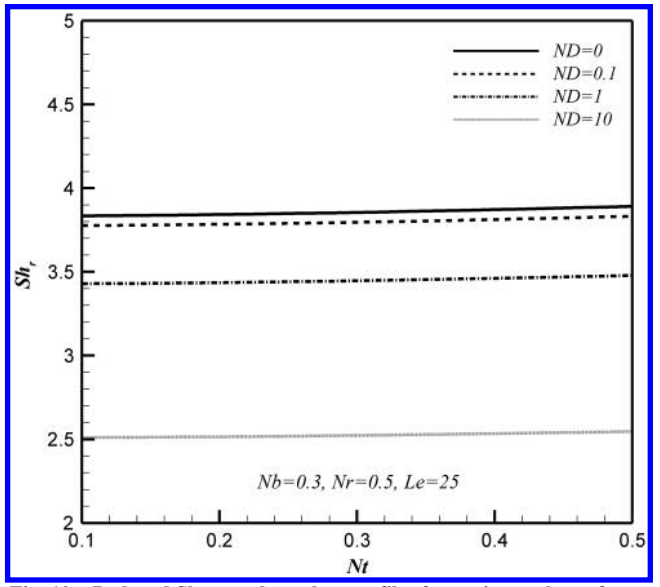

Fig. 10 Reduced Sherwood number profiles for various values of non-Darcy parameter (ND) and thermophoresis parameter (Nt) for $Le = 25$.

Increase of non-Darcy parameter decreases the magnitude of concentration gradient on the wall surface, which in turn results in the decrease of reduced Sherwood number (Figs. 9 and 10).

V. Conclusions

A combined similarity and numerical approach is used to theoretically investigate the natural convection about a vertical cone embedded in a nanofluid saturated porous medium using the Forchheimer-extended Darcy equation. The concentration gradient due to thermophoresis and Brownian motion is also taken into account. The results of present study are as follows:

1) Increase of non-Darcy parameter increases the temperature and concentration profiles but decreases the velocity profile.

2) Increase of non-Darcy parameter decreases the reduced Nusselt number and the reduced Sherwood number.

3) Increase of thermophoresis parameter decreases the reduced Nusselt number, but it does not have a significant effect on the reduced Sherwood number.

4) As Lewis number increases, the magnitude of the reduced Nusselt and Sherwood numbers would also increase.

5) The increase in the non-Darcy parameter has a significant effect on the shape of velocity, temperature and concentration profiles. It is found that the curvature of the velocity, temperature, and concentration profiles is reduced by increase of non-Darcy parameter.

Acknowledgments

The authors are grateful to the Shahid Chamran University of Ahvaz for its support through this paper. They would like to thank the anonymous referees for their constructive comments and Mehdi Ghalambaz for his valuable advice on the revision of the paper.

References

[1] Das, S. K., Choi, S. U. S., Yu, W., and Pradeep, T., *Nanofluids-Science and Technology*, Wiley, Hoboken, NJ, 2007, pp. 1–37.

[2] Cheng, P., Le, T. T., and Pop, I., "Natural Convection of a Darcian Fluid About a Cone," *Internationl Communications in Heat and Mass Transfer*, Vol. 12, No. 6, 1985, pp. 705–717. doi:10.1016/0735-1933(85)90023-5

[3] Nield, D. A., and Bejan, A., *Convection in Porous Media*, 3rd ed., Springer–Verlag, New York, 2006, pp. 1–13.

[4] Yih, K. A., "The Effect of Uniform Lateral Mass Flux on Free Convection About a Vertical Cone Embedded in a Aaturated Porous Media," *International Communications in Heat and Mass Transfer*, Vol. 24, No. 8, 1997, pp. 1195–1205. doi:10.1016/S0735-1933(97)00114-0

[5] Yih, K. A., "Radiation Effect on Mixed Convection over an Isothermal Cone in Porous Media," *Journal of Heat and Mass Transfer*, Vol. 37, No. 1, 2001, pp. 53–57. doi:10.1007/s002310000132

[6] Grosan, T., Postelnicu, A., and Pop, I., "Free Convection Boundary Layer over a Vertical Cone in a non-Newtonian Fluid Saturated Porous Medium with Internal Heat Generation," *Technische Mechanik*, Vol. 14, No. 4, 2004, pp. 91–104.

[7] Ramanaiah, G., and Malarvizhi, G., "Free Convection about a Wedge and a Cone Subjected to Mixed Thermal Boundary Conditions," *Acta Mechanica*, Vol. 93, Nos. 1–4, 1992, pp. 119–123. doi:10.1007/BF01182577

[8] Chamkha, A. J., Bercea, C., and Pop, I., "Free Convection Flow over a Truncated Cone Embedded in a Porous Medium Saturated with Pure or Saline Water at Low Temperatures," *Mechanics Research Communications*, Vol. 33, No. 4, 2006, pp. 433–440. doi:10.1016/j.mechrescom.2005.10.001

[9] Sohouli, A. R., Domairry, D., Famouri, M., and Mohsenzadeh, A., "Analytical Solution of Natural Convection of Darcian Fluid About a Vertical Full Cone Embedded in Porous Media Prescribed Wall Temperature by Means of HAM," *International Communications in Heat and Mass Transfer*, Vol. 35, No. 10, 2008, pp. 1380–1384. doi:10.1016/j.icheatmasstransfer.2008.08.008

[10] Cheng, C. Y., "Natural Convection Heat and Mass Transfer from a Vertical Truncated Cone in a Porous Medium Saturated with a non-Newtonian Fluid with Variable Wall Temperature and Concentration," *Internationl Communications in Heat and Mass Transfer*, Vol. 36, No. 6, 2009, pp. 585–589. doi:10.1016/j.icheatmasstransfer.2009.03.011

[11] Cheng, C. Y., "Soret and Dufour Effects on Natural Convection Heat and Mass Transfer from a Vertical Cone in a Porous Medium," *Internationl Communications in Heat and Mass Transfer*, Vol. 36, No. 10, 2009, pp. 1020–1024. doi:10.1016/j.icheatmasstransfer.2009.07.003

[12] Vasantha, A., Pop, I., and Nath, G., "Non-Darcy Natural Convection over a Slender Vertical Frustum of a Cone in a Saturated Porous Medium," *Internationl Journal of Heat and Mass Transfer*, Vol. 29, No. 1, 1986, pp. 153–156. doi:10.1016/0017-9310(86)90043-8

[13] Nakayama, A., and Pop, I., "A Unified Similarity Transformation for Free, Forced and Mixed Convection in Darcy and Non Darcy Porous Media," *Internationl Journal of Heat and Mass Transfer*, Vol. 34, No. 2, 1991, pp. 357–367. doi:10.1016/0017-9310(91)90256-E

[14] Nakayama, A., Kokudai, T., and Koyama, H., "An Integral Treatment for Non-Darcy Free Convection over a Vertical Flat Plate and Cone Embedded in a Fluid-Saturated Porous Medium," *Warme-und*

Stoffubertragung, Vol. 23, No. 6, 1988, pp. 337–341.
doi:10.1007/BF01650469

[15] Cheng, C. Y., "Non-Darcy Natural Convection Heat and Mass Transfer from a Vertical Wavy Surface in Saturated Porous Media," *Applied Mathematics and Computation*, Vol. 182, No. 2, 2006, pp. 1488–1500.
doi:10.1016/j.amc.2006.05.037

[16] Ahmad, S., and Pop, I., "Mixed Convection Boundary Layer Flow from a Vertical Flat Plate Embedded in a Porous Medium Filled with Nanofluids," *International Communications in Heat and Mass Transfer*, Vol. 37, No. 8, 2010, pp. 987–991.
doi:10.1016/j.icheatmasstransfer.2010.06.004

[17] Hady, F. M., Ibrahim, F. S., Abdel Gaied, S. M., and Eid, M. R., "Effect of Heat Generation/Absorption on Natural Convective Boundary-Layer Flow from a Vertical Cone Embedded in a Porous Medium Filled with a non-Newtonian Nanofluid," *International Communications in Heat and Mass Transfer*, Vol. 38, No. 10, 2011, pp. 1414–1420.
doi:10.1016/j.icheatmasstransfer.2011.07.008

[18] Nield, D. A., and Kuznetsov, A. V., "The Cheng–Minkowycz Problem for Natural Convective Boundary Layer Flow in a Porous Medium Saturated by a Nanofluid," *International Journal of Heat and Mass Transfer*, Vol. 52, Nos. 25–26, 2009, pp. 5792–5795.
doi:10.1016/j.ijheatmasstransfer.2009.07.024

[19] Gorla, R. S. R., Chamkha, A. J., and Rashad, A. M., "Mixed Convective Boundary Layer Flow over a Vertical Wedge Embedded in a Porous Medium Saturated with a Nanofluid: Natural Convection Dominated Regime," *Nanoscale Research Letters*, Vol. 6, No. 1, March 2011, pp. 1–9.
doi:10.1186/1556-276X-6-207

[20] Rashad, A. M., El-Hakiem, M. A., and Abdou, M. M. M., "Natural Convection Boundary Layer of a non-Newtonian Fluid about a Permeable Vertical Cone Embedded in a Porous Medium Saturated with a Nanofluid," *Computers and Mathematics with Applications*, Vol. 62, No. 8, 2011, pp. 3140–3151.
doi:10.1016/j.camwa.2011.08.027

[21] Keller, H. B., "Numerical Solution of Two-Point Boundary Value Problems," *SIAM Regional Conference Series in Applied Mathematics*, J. W. Arrowsmith Ltd., Bristol, England, U.K., 1976.

[22] Russell, R. D., and Shampine, L. F., "A Collocation Method for Boundary Value Problems," *Numerical Mathematics*, Vol. 19, No. 1, 1972, pp. 1–28.
doi:10.1007/BF01395926

[23] Chamkha, A., Gorla, R. S. R., and Ghodeswar, K., "Non-Similar Solution for Natural Convective Boundary Layer Flow over a Sphere Embedded in a Porous Medium Saturated with a Nanofluid," *Transport in Porous Media*, Vol. 86, No. 1, 2011, pp. 13–22.
doi:10.1007/s11242-010-9601-0

[24] Gorla, R. S. R., and Chamkha, A. J., "Natural Convective Boundary Layer Flow over a Horizontal Plate Embedded in a Porous Medium Saturated with a Nanofluid," *Journal of Modern Physics*, Vol. 2, No. 2, 2011, pp. 62–71.
doi:10.4236/jmp.2011.22011

[25] Cheng, P., Ali, C. L., and Verma, A. K., "An Experimental Study of non-Dacian Effects in Free Convection in a Saturated Porous Medium," *Letters in Heat and Mass Transfer*, Vol. 8, No. 4, 1981, pp. 261–265.
doi:10.1016/0094-4548(81)90040-0

[26] Buongiorno, J., "Convective Transport in Nanofluids," *Journal of Heat Transfer*, Vol. 128, No. 3, 2006, pp. 240–250.
doi:10.1115/1.2150834

[27] Zheng, F., "Thermophoresis of Spherical and Non-Spherical Particles: A Review of Theories and Experiments," *Advances in Colloid and Interface Science*, Vol. 97, Nos. 1–3, 2002, pp. 255–278.
doi:10.1016/S0001-8686(01)00067-7